

TEMPERATURE STRUCTURE OF METAL ENRICHED NOVAE

BELAY SITOTAW GOSHU

Department of Physics
Dire Dawa University
Dire Dawa
P.O. Box 1362
Ethiopia

Department of Mathematics, Computing & Astronomy
University of South Africa
Pretoria
P.O. Box 392
South Africa
e-mail: belaysitotaw@gmail.com

Abstract

We have constructed a model to study the ionization structure of electron temperature with the basic parameters of blackbody temperature of the order of 10^5 K and with the solar abundances of heavy metals. The goal of the present investigation is to provide impacts of chemical abundances on structure of temperature, electron density, and temperature fluctuations. This model consists of six metallicities. The average logarithmic abundances (relative to H = 12.00) are He: 11.00, C: 8.43, N: 7.83, O: 8.69, and Ne: 7.69. Abundances of C, N, O, and Ne changes by scale factor 10 and 100. Since, in classical novae ejecta are characteristically enriched in C, N, O, Ne abundances. We have looked into correlations between metal abundances and temperature of electrons by changing abundances of heavy metals and using photoionization modelling codes cloudy. The result revealed that the higher increment the abundances of

Keywords and phrases: stars: novae-stars, abundances, photoionization, UV.
Received June 19, 2016

heavy metals, the lower the electron temperature and shifted to the inner region of He^{+2} edges. It also suggested that the electron number density changes with abundances of the most primary elements like C, N, O, and Ne.

1. Introduction

The ionization equilibrium at each point in the nebulae is fixed by the balance between photoionization and recombination of electrons with the ions. Since hydrogen is the most abundant element, we can get a first idealized approximation to the structure of nebulae by considering a pure H cloud surrounding a single hot star (Osterbrock [9]; Osterbrock & Ferland [10]). The ionization equilibrium equation is helping to get the temperature of plasma by balancing the energy gains and the energy loss. In most of ionized plasma, the energy input comes from a flux of UV radiation which photoionized the ions and in the process imparts kinetic energy to the ionized components to change the electron temperatures.

The energy balance between ionizational heating and cooling processes by electrons recombination, gas expansion, collisionally excited forbidden lines of several atoms and free-free radiation of hydrogen is solved. The radiation of the field of classical novae is given by a synthetic spectrum calculated on the assumption of spherical symmetry and time independent, expanding non-local thermodynamic equilibrium in radiative equilibrium (Beck et al. [1]).

The ionization equilibrium equation describes the spatial dependence of the state of ionization in expanding spherically symmetric homogeneous hydrogen shell surrounding a central star. It will be assumed that the shell is ejected by central star. The expansion of the shell can be considered to be a consequence of the fact that the shell is ejected by the central star. Here we assumed the shell is moving with constant velocity (Bosma [2]).

Photoionized gas is also found around novae. Novae stars that have undergone sporadic outbursts and they are surrounded by faint shells of ejected gas that have been ejected from the parent star as it evolved to its final white dwarf stage. Because the core of the parent star is more highly ionized that are emission nebulae and has a distinctive spectrum (Dalgarno & Lepp [3]).

An expanding gaseous shell around the central stellar systems helps to produce low gas temperature. This is possible by using large heavy metal enhancement in the processes, which is compared with the solar abundances used by Smith [19]. In order to get reliable result, we enhanced the abundances of heavy metals given by Serenellil et al. [18] by scale factor 10 and 100. We assumed such enhancement of heavy metals is capable of cooling the gas very efficiently. One of the most important metals which play a great role for cooling temperature is oxygen. In this work, we also assessed the impacts of other primary elements like C, N, and Ne by enhancing the same factor.

The present study is less ambitious than the works of Smith [19], but it concerns a closely related topic and we believe that our work is a step in the direction that they advocate. Understanding of temperature electron density fluctuations in novae shell is a key problem in the computation of chemical abundances, which allows on a variety fundamental issues in Astrophysics.

The goal of this study includes a reassessment of the ionization structure of temperature and electron density and to understand the impacts of heavy metals on the fluctuations of electron temperature. To do so the abundances of we change the abundances of carbon, oxygen, nitrogen, and neon by scale factor 10 and 100, like what was done by Smith [19]. We advocate cloudy c13.03 to solve this problem (Ferland et al. [5]). It then computes the ionization structure of elements, temperatures, and electron density.

In Section 2, we describe the model and the method of solution used. In Section 3, a discussion of some of the results follows and then we proceed to the conclusion part of the paper in the last section.

2. Models

The model consists of six metallicities. But the ejected novae are enriched in C, N, O, Ne and other elements like Mg, Si, and S. We mainly give attention of the most primary elements whose abundances are given by Serenellil et al. [18]; Pontefract and Rawlings [13]. Therefore, in this work, we change abundances of carbon, nitrogen, oxygen, and neon by factors of 10 and 100, in order to study the impacts on ionization structure of both electron temperature and density. The other elements like Mg, Si, and S are neglected. Initially, the chemical abundances were taken from the revisited solar values given by Serenellil et al. [18]. Very recently, Serenellil et al. [18] have done a complete revision of the solar photospheric abundances for nearly all elements. Therefore, we used this revised abundances of He, C, N, O, and Ne shown in Table 1. As it is already shown the abundances in Serenellil et al. [18] agree with photospheric abundances very well, and they could have potential impact on the ionization structure.

The geometry of our model novae shell is constant density ($n(\text{H}) = 2000\text{cm}^{-3}$), in one hand and non-uniform hydrogen density which vary with position in the other hand, spherical gas with the filling factor ϵ . The ionizing cluster is treated as a point source of the gas cloud. The photoionization calculation stopped when the temperature is lower than 100K. We define differing geometries by varying the filling factor.

Table 1. Adopted solar chemical compositions used in this model

Elements	Abundances ¹
He	11.0
C	8.43
N	7.83
O	8.69
Ne	7.69

¹Abundances given as $\epsilon_i = \log N_i / N_H$ (Serenellil et al. [18]).

The physical processes included in the code are: photoionization, collisional ionization, dielectronic recombination, and charge exchange reactions. Given these processes, the ionization and thermal structure of the plasma is evolved from an initial state assumed to have a temperature of $T = 10^5 \text{K}$ and equal ionization fractions in each state.

We have generated cloudy photoionization models assuming abundances of elements given by Serenellil et al. [18]. This is used as the initial comparison revealed to see the ionization structure of both electron density and temperature before we test the impacts of metal enriched novae. Interestingly, in photoionized gas, the ionization structure of both electron density and temperature are produced by heavy metals like carbon, oxygen, and nitrogen. Hence, the strength of these features is quite sensitive to elemental abundances.

The computations were carried out by using the treatment of cloudy codes initially developed by Ferland et al. [5] to model the ionization structure from photoionization of the novae shell. As it was assumed by Smith [19], charge exchange and dielectronic reactions were included in the model, as well as photoionization by x-rays. To make the model with cloudy, we set the radiation field at a certain time to be a blackbody with $T_{\text{eff}} = 10^5 \text{K}$ and radius of the star is $\log r = 9.37 \text{ R(sun)}$ and uniform and non-uniform hydrogen density sphere model and the filling factor in the novae shell.

We delineate deferring geometries by varying the filling factor with the position defined in Equation (1) cloudy allows the filling factor to vary with radius through the shell is given by Schwarz et al. [15]

$$f(r) = f(r_0) \left(\frac{r}{r_0} \right)^{-\alpha}, \quad (1)$$

where r_0 is the inner radius and α is the exponent of the power law, and as we know the dust grains have impact on the temperature of electrons, through heating by photoelectric effect, we do not include the effect of dust grain in this work.

2.1. Ionization model

We assumed that most of the material initially forming the accretion disk of the white dwarf is ejected in the first phase of the novae event. The initial radius of the shell $\log(r) = 13\text{cm}$ and a constant shell velocity of 400kms^{-1} . The particle density diluted by the power law as shell expands. We consider models with initial density $n(\text{H}) = 2000\text{cm}^{-3}$. The photoionization rate Q_i can be calculated with the shell for atoms species i are performed using

$$Q_i = \int_{\nu_i}^{\infty} \frac{4\pi\sigma_i}{h\nu} J_\nu d\nu, \quad (2)$$

where J_ν is the mean intensity of radiation with frequency ν , σ_i is the ionization cross-section, ν_i is the initial threshold frequency for photoionization, and h is the Planck constant.

The intensity of radiation was divided into stellar J_s and diffused J_d components on different frequency grids. Thus,

$$J_\nu = J_s + J_d. \quad (3)$$

The stellar radiation decreases outward because of geometrical dilution and absorption, and since its only source can be written as

$$4\pi J_\nu = \pi F_{\nu s}(r) = \pi F_{\nu s}(R) \left(\frac{R}{r}\right)^2 e^{-\tau_\nu}, \quad (4)$$

where $\pi F_{\nu s}(r)$ is the standard astronomical notation for the flux of stellar radiation (per unit area per unit frequency per unit time) at r , $\pi F_{\nu s}(R)$ is the flux at radius of stellar R , and τ_ν is the radial optical depth at r (Osterbrock & Ferland [10]),

$$\tau_\nu = \int_0^r k_\nu dr, \quad (5)$$

where $k_\nu = N_0(\text{H})a_\nu$ and a_ν is the ionization cross-section of ions.

The equation for diffused stellar radiation (Smith [19]) for the entire volume of shells is given by

$$J_v^d = \int J_v(r) e^{-\tau_v} dV. \quad (6)$$

3. Results and Discussions

We have tried to test this model for uniform hydrogen density throughout the nebulae using the same input parameters used by Smith [19] and photoionization codes.

We have generated cloudy photoionization model for uniform hydrogen density on the novae shell assuming the abundances (Serenellil et al. [18]). This is our initial comparison revealed to see the ionization structure of both electron density, temperature and the ionization structure of hydrogen and helium before we testing the impacts of metal enriched novae. Since the ionization structure of nebulae is mainly determined by the ionizing radiation field and by the nebular geometry (Schwarz et al. [15]). It is not only governed by the spectra energy distribution of the stellar radiation field or filling factor but also by the importance of recombination and charge exchange reactions. Interestingly, in photoionized gas, the ionization structure of heavy metals like carbon, nitrogen, and oxygen when enhanced by 10 and 100 and we primarily observed the recombination of He^{+2} into He^+ in the inner region to change the temperature of electron and density.

Our model contained Ne but this was neglected by Smith [19] and values of abundance were taken from Serenellil et al. [18]. The ionization structure of hydrogen and helium is shown in Figure 1. The H^+ to H^0 transition resembles the edge of the so-called Stromgren sphere and is brought about physical processes. In the Figure 1 shown, the H^+ line drops to a point where it begins to level off as a result, in part, of ionization by diffuse photons from the recombination of He^+ to He^0 (MacAlpine [7]).

He^+ , along with a number of positive ions, is dominant in the outer part of the nebulae where hydrogen exists in H^0 . The input radiation spectrum, though cut down absorbed appreciable at high frequencies, still supplies enough photons to ionize other elements. This occurs because the absorption cross-sections for most slowly with frequency than do hydrogenic cross-sections (MacAlpine [7]). Besides, the result shows that Stromgren radius of He^+ is greater than H. This is due to the energy of the ionizing spectrum.

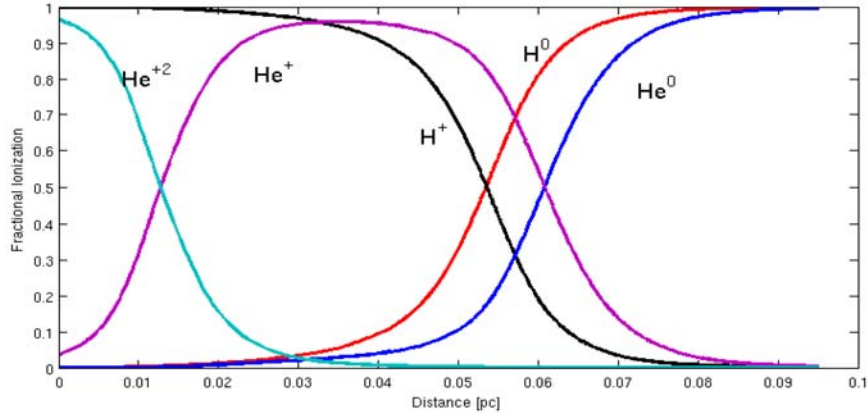


Figure 1. The ionization structure of hydrogen and helium computed with the photoionization codes.

The ionization structures of electron temperature and density profile are shown in Figure 2. The curve is similar, but the electron temperatures of this model is higher than the previous model (the previous model $T_e = 1.72 \times 10^4 \text{K}$ and this model $T_e = 1.883 \times 10^4 \text{K}$, it changes by 18%). Where OIII (the most efficient coolant) is suppressed, T_e will rise dramatically. Furthermore, this higher T_e can slightly change the ionization structure of H and He by making recombination less efficient. Since the highest energy photons are selectively attenuated as the radiation propagates outward. The electron density structure shown in lower panel of Figure 2 depends radically and falls down with distance from the center.

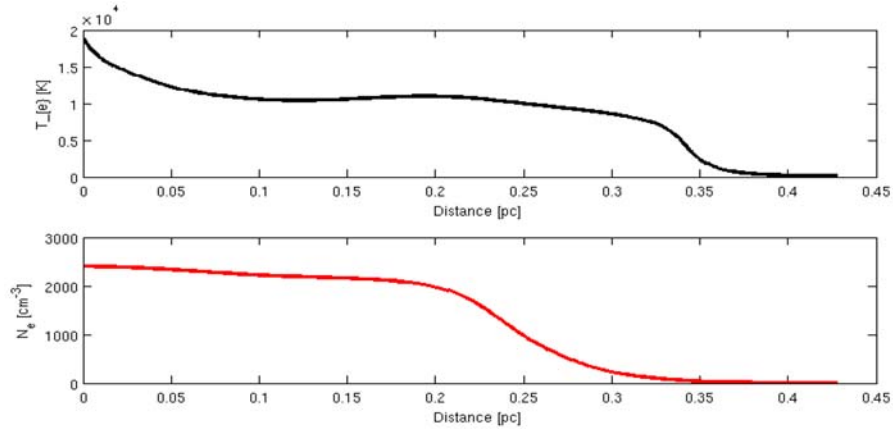


Figure 2. The ionization structure of temperature and electron density before we test metal enriched novae using chemical abundances shown in Table 1 and photoionization codes.

The Figure 3 shows change of electron temperature as function of metallicity. Fluctuations of electron temperatures are not the same for each element. They have their own identity. The fluctuation of electron temperature is highly affected when the abundances of nitrogen changed by scale factor of 10 than 100. They have an impact on cooling electron temperature on the ionic distribution. Relative to oxygen the cooling effect is negligible. As it is shown in Figure 4, the electron temperature produced by oxygen abundance is lower when it is changed by scale factor 100. The lowest temperature was observed in the case of hundred fold enhancement of oxygen, the temperature at the inner radius 576K. This is because of primarily to the cooling efficiency of the OIV 25.9 μm line. Thus, the cooling rates for plasma in collisional ionization equilibrium can be conveniently tabulated as a function of the temperature and composition (metallicity) of the gas (Robert et al. [14]).

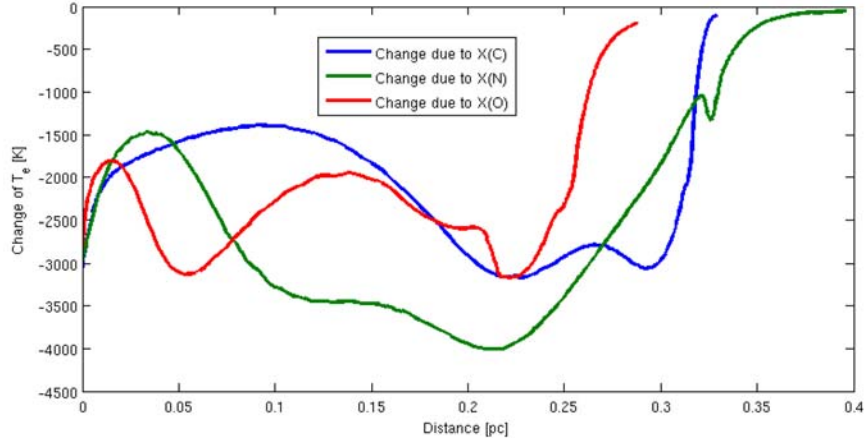


Figure 3. The ionization structure of temperature variation with the metal enriched abundances when the abundance of carbon, nitrogen, and oxygen are raised by 10 and 100. The other abundances remain the same shown in Table 1.

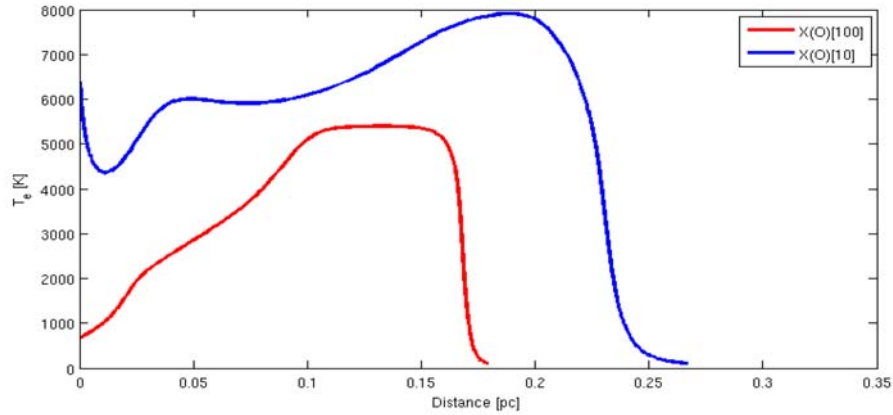


Figure 4. The ionization structure of temperature profiles with the metal enriched abundances when $X(O)$ is raised by 10 and 100. The other abundances remain the same as shown in Table 1.

The flux of $[OIV] \lambda 25.9\mu m$ line relative to $H\beta$ is 2.096. The slow rise in temperature from 576K to 5438K at distance of 0.047pc and it is due to decrease of $OIII$ abundances, and hence a decrease in the cooling. The

electron temperature sharply falls down to the minimum temperature in the outer region. The electron temperature was calculated by Smith [19] in the inner shell was 700K. There is significant variation of electron temperature in the inner shell this is due primarily to the neon abundance included in this work.

In all cases, when abundances of carbon, nitrogen, and oxygen enhanced by 10 and 100 scale factors, the electron temperature drops as the abundances change. But the intensities of the most prominent oxygen lines are correlated with metallicity due to the shifting of the cooling from the optical forbidden lines to the infrared as the electron temperature drops with increasing abundance of coolants.

As it is shown in Figure 5, the electron temperature for nitrogen abundances changed by scale factor 10 is greater than carbon abundance changed by similar factor and similar for 100 scale factor. This result confirms that electron temperature depends on change of abundances. As the abundances of elements increases, temperature of electrons is decreased due to cooling processes. Therefore, increasing either carbon or nitrogen abundances to the same concentration of oxygen, the effects are not as remarkable as that of oxygen abundances.

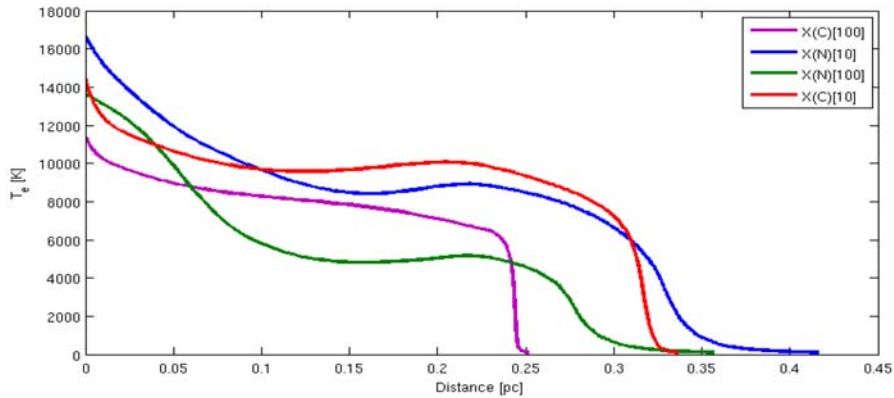


Figure 5. The ionization structure of temperature variation with the metal enriched abundances. When abundances of carbon and oxygen are raised by 10 and by 100 separately. The other abundances remain the same as shown in Table 1.

Our result confirm that the electron temperature as a function of metallicity. At very low abundances, there is little coolant and the gas is hot. But at high abundances, there are enough coolants to lower the temperature of the gas, i.e., as a number of coolants are increasing, the temperature declines and the cooling burden shifts to the more excited infrared lines (McGaugh [8]). As a result of shifting the coolant, the ratio of the line is very sensitive.

Our result also tells that there is variation of electron density due to abundances of elements as it is shown in Figure 6. The electron density mainly depends on hydrogen and helium abundances. The contribution of the other heavy metals is negligible. But in this work, because of change of enhancement of abundances by 10 and 100 factors affect the density. In the input parameters of abundances shown in Table 1, the relative abundances of oxygen is greater than the other heavy metals, density of electron when oxygen enhanced by 100 is greater than the rest.

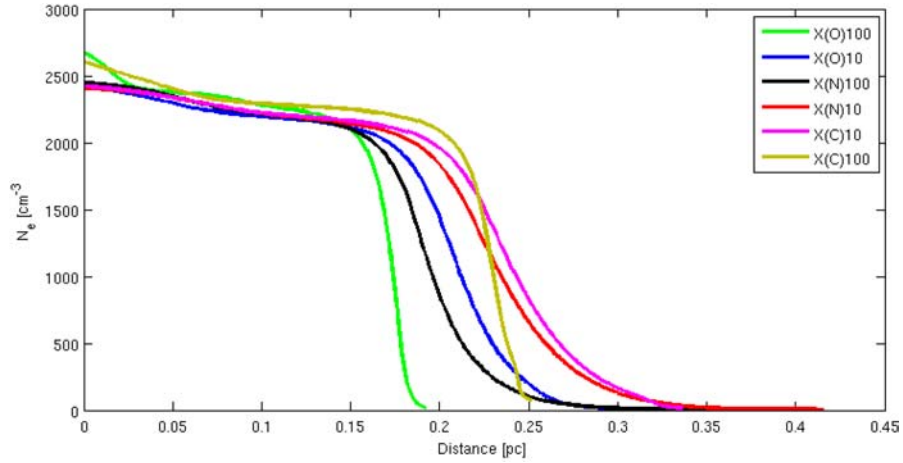


Figure 6. The electron density with the metal enriched abundances when abundances of carbon, nitrogen, and oxygen are raised by 10% and by 100% separately. The other abundances remain the same as shown in Table 1.

The ionization structure of electron temperature when Ne abundances is enhanced by 10 and 100 shown in Figure 7. The results confirms that as the abundances of oxygen is enhanced by 10, the electron temperature rises slowly from 1.3×10^4 K to 1.37×10^4 K and falls sharply. The structure has different feature when it is enhanced by 100 fold. The electron temperature sharply rises from 2.54×10^3 K to 7.1×10^3 K and falls down to 2.19×10^3 K. There is a fluctuation of electron temperature due to enhancement of Ne abundances. This is due to emission lines of $\text{Ne}\lambda\lambda 3869; 3968$ produced on this enhancement is lower than 10 fold abundances of Ne. Therefore, these lines produced a lower temperature because it has cooling impacts.

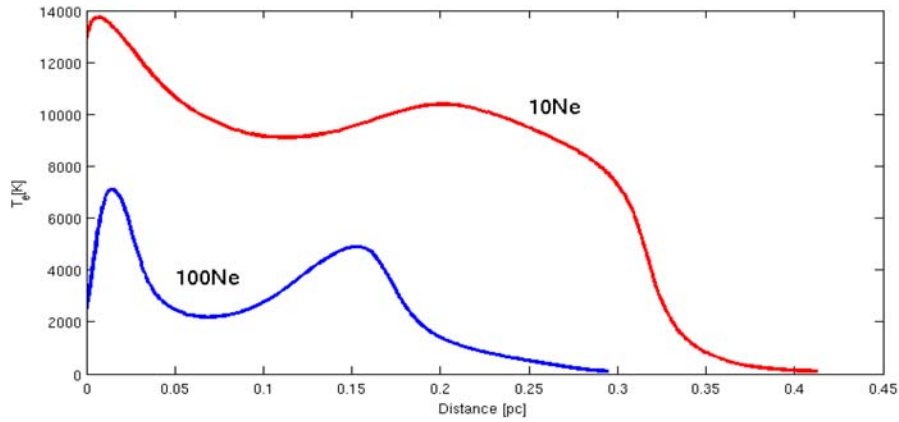


Figure 7. The electron temperature for metal enriched abundances of neon by 10% and by 100% separately. The other abundances remain the same as shown in Table 1.

OII permitted and [OII] forbidden lines can be used to infer a values of t^2 as has been done by Esteban et al. [4] for the nebulae. Peimbert [11] characterizes the temperature structure of gaseous nebulae to a second order approximation by two parameters: The average temperature T_0 , and the root mean square temperature fluctuation, t^2 , given by the following expression for an ion of abundances N_i :

$$T_0(N_e, N_i) = \frac{\int T_e(r) N_e N_i dV}{\int N_e N_i dV}, \quad (7)$$

and

$$t^2 = \frac{\int (T_0 - T_e)^2 N_e N_i}{T_0^2 \int N_e N_i dV}, \quad (8)$$

where N_e and N_i are the electron and ion density distribution and V is the volume.

Abundances discrepancies have used to explain temperature fluctuations in the novae shell. This fluctuations t^2 , first defined or introduced by Peimbert [11], have been popular in explaining the differences in abundances found from forbidden lines shown in Table 2. The temperatures of [OIII] highly depend on the enhancement of chemical abundances by 10 and 100, increased by 54%. But the temperature fluctuations changed by 58%. As we can see from the Table 2, the temperature of [OIII] also depends on the abundances of carbon and nitrogen enhancement. In both cases, the temperature decreases when they are enhanced by 10 and 100 scale factors. The temperature of HII is highly depends on the enhancement of abundances. The inferred temperature fluctuations when oxygen enhanced by 100 is less than nitrogen enhanced by the same factor. Since oxygen abundances lowered the electron temperature and rises outward because of the forbidden lines OIII.

Table 2. Dependence of output temperature and square temperature fluctuation with chemical abundances of oxygen, carbon, and nitrogen through the novae shell

Element	$\log\left(\frac{X_i}{H}\right)$	$T_e[\text{OIII}]\text{K}$	$T_e[\text{HII}]\text{K}$	$t^2[\text{OIII}]$	$t^2[\text{HII}]$
C	8.43	11000	10700	0.0032	0.0045
	9.43	9970	9580	0.0017	0.0012
	10.43	8400	7270	0.0085	0.0031
N	8.83	10100	8640	0.014	0.015
	9.83	9100	5090	0.074	0.092
O	9.61	7530	6040	0.0024	0.0017
	10.61	16400	3390	0.058	0.081
Ne	8.69	9800	9570	0.0037	0.0044
	9.69	19000	2860	0.096	0.088

In all cases the structural temperature $T[\text{OIII}] > T(\text{H}^+)$. The temperature of $T[\text{OIII}]$ is weighted since it is produced in the hot regions of the novae, while the coulomb interaction during the recombination process which produces the Balmer emission is more efficient for low kinetic energy electrons. The other case is that $T(\text{HII})$ is in the region of hot ionized novae $T(\text{H}^+)$ samples of it, and in the inner region where the oxygen ionized into O^{+3} and higher, therefore temperature of OIII is greater than the temperature of HII (Zhang et al. [20]).

As Beck et al. [1] summarized the range values found for the square of temperature fluctuations found by Equation (7) from observations, $0.01 \leq t^2 \leq 0.09$. Therefore, our results revealed on this interval. When oxygen enhanced by 100 fold, $t^2(\text{O}^{+2})$ is almost agree with peak values of the square of temperature fluctuations. Similarly, $t^2(\text{O}^{+2})$ produced by enhancement of nitrogen abundances, its value slightly the expected values.

The ionic abundances of O and N are used to determine the effective temperatures of ions. The ratio of ionizing photons could determine the temperature. The value of electron temperature can be calculated from the intensity ratios $\frac{I(\lambda 5007 + \lambda 4959)}{I(\lambda 4363)}$ and $\frac{I(\lambda 6548 + \lambda 6584)}{I(\lambda 5755)}$. This equation was first formulated by Seaton [17]. The temperatures of ions given by the ratio of ions are shown in Table 3. The lines ratio of [OII] depends strongly with abundances. The observed result is shown in the width of H β decreases with abundances (Searle [16]). The intensity optical oxygen line steadily decreases with increasing metallicity of oxygen. As we can see from Table 3, when carbon and nitrogen enhanced by 10 and 100, the intensity ratio of oxygen lines is increased with the metallicity.

As we can see from the ratio of intensity line given by $\frac{I(\lambda 5007 + \lambda 4959)}{I(\lambda 4363)}$ is lowest relative to other when the abundances of oxygen enhanced by 100. It also shows that the temperature of electron of [OIII] ion calculated from the photoionization model code is greater than the one calculated from the ratio of lines shown in Table 3. Similarly, we tried to calculate the temperature of [NII] when the abundances of oxygen is enhanced by 100, but it does not exist. The line intensity of emission line is [NII] $\lambda 5755$ does not appear.

Table 3. Dependence of temperature of ions with chemical abundances of oxygen, carbon, and nitrogen enhanced by 10 and 100 through the novae shell

Element	Abundances	$\frac{I(\lambda 5007 + \lambda 4959)}{I(\lambda 4363)}$	$\frac{I(\lambda 6548 + \lambda 6584)}{I(\lambda 5755)}$
C	8.43	148.35	75.59
	9.43	202.88	92.37
	10.43	374.94	199.34
N	8.83	191.63	127.29
	9.83	258.98	655.36
O	9.61	610.39	192.15
	10.61	610.39	–

4. Conclusion

We have constructed an extensive model of temperature structure of metal enriched novae. The ionization structure of electron temperature and its fluctuations was modelled using photoionization equilibrium, cloudy. This was done by enhancing abundances of carbon, nitrogen, and oxygen by scale factor 10 and 100. The chemical abundances of the other elements were taken fixed as the nominated elements changes by 10 and 100. We have used the same inputs as Harrington [6] for effective temperature of star as $T_{\text{eff}} = 10^5 \text{K}$, $\log R(\text{sun}) = 9.37 \text{cm}$ and hydrogen density 2000cm^{-3} . The filling factor of across the shell depends on the radial distance.

Our result confirms that in this model, oxygen is by far the most important for determining the electron temperature structure. This does not mean that carbon and nitrogen make non negligible contribution in electron temperature structure. The concept of temperature fluctuations associated with the chemical abundances of elements. The higher the abundances the lower will be the temperatures. But the intensities of the most prominent oxygen lines are correlated with metallicity due to the shifting of the cooling from the optical forbidden lines to the infrared as the electron temperature drops with increasing abundance of coolants.

The result also confirms that the temperature of HII is highly depending on the enhancement of chemical abundances. Thus, the cooling rates for plasma in collisional ionization equilibrium can be dependent as a function of the temperature and composition (metallicity) of the gas (Robert et al. [14]).

As Beck et al. [1] summarized the range values of found for the square of temperature fluctuations by Equation (7) from observations lies in, $0.01 \leq t^2 \leq 0.09$. Therefore our results that are shown in Table 2 revealed on this interval. The intensity of optical oxygen lines steadily

decrease with increasing metallicity of oxygen. As we can see from Table 3, when carbon and nitrogen enhanced by 10 and 100, the intensity ratio of oxygen lines is increased with the metallicity. Therefore, when abundances of the metallicity strongly depends with the intensity ratios of ions.

References

- [1] H. K. B. Beck, P. H. Hauschildt, H. P. Gali and E. Sedlmayr, Ionization and temperature of novae shell, *A&A* 294 (1995), 195.
- [2] P. B. Bosma, the state of ionization in novae shell, *A&A* 40 (1975), 175.
- [3] A. Dalgarno and S. Lepp, *Atomic, Molecular and Optical Physics Handbook*, Edited by Drake G., W., F., AIP Press, New York, 1996.
- [4] C. Esteban, M. Peimbert, J. Garcia-Rojas, M. T. Ruiz, A. Peimbert and M. Rodriguez, 2004, Carbon and oxygen galactic gradients I: Observational values from H II region recombination lines, *MNRAS* 335 (1998), 229.
- [5] G. J. Ferland et al., *Hazy: Introduction to Cloudy c13.03*, 2013.
- [6] J. P. Harrington, Ionization stratification and chemical abundances in the planetary nebulae, *Astrophys. J.* 156 (1969), 903.
- [7] G. M. MacAlpine, Photoionization model for the emission line regions of quasi-stellar and related objects, *ApJ* 175 (1972), 11.
- [8] S. S. McGaugh, H II region abundances: Model oxygen line ratios, *ApJ* 380 (1991), 140.
- [9] D. E. Osterbrock, *Astrophysics of Gaseous Nebulae and Active Galactic Nuclei*, California University of Science Book, 1989.
- [10] D. E. Osterbrock and G. J. Ferland, *Astrophysics of Gaseous Nebulae and Active Galactic Nuclei*, 2nd Edition, University Science Books, 2005.
- [11] M. Peimbert, Temperature determinations of H II regions, *ApJ* 150 (1967), 825.
- [12] M. Peimbert, In the Analysis of Emission Lines, *Proceedings of the Space Telescope Science Institute Symposium Number 8*, Editors R. Williams & M. Livio (Cambridge CUP), 165, 1995.
- [13] M. Pontefract and J. M. C. Rawlings, The early chemical evolution of nova outflows, *MNRAS* 347 (2004), 1294.
- [14] P. C. Robert, R. P. C. Wiersma, J. Joop Schaye, D. Britton and B. D. Smith, 2008, arXiv:0807.3748v2 [astro-ph].
- [15] G. J. Schwarz, S. Starrfield, S. N. Shore and P. H. Hauschildt, Abundance analysis of the slow nova PW Vulpeculae 1984, 1997, arXiv:astro-ph/9705086v1.

- [16] L. Searle, Evidence for composition gradients across the disks of spiral galaxies, *ApJ* 168 (1971), 327.
- [17] M. J. Seaton, *MNRAS* 189 (1968), 129.
- [18] A. M. Serenelli, S. Basu, J. W. Ferguson and M. Asplund, New solar composition: The problems with solar models, *ApJ* 705 (2009), L123.
- [19] D. P. Smith, Photoionization model of metal enriched novae shell, *MNRAS* 248 (1991), 217.
- [20] Y. Zhang, W. Liu, R. Wesson, P. J. Storey, Y. Liu and I. J. Danziger, Electron temperature and densities of planetary nebulae determined from the nebular hydrogen recombination spectrum and electron density, *MNRAS* 351 (2004), 935.

